KURENAI 紅
Kyoto University Research Information Repository

KYOTO UNIVERSITY

| | |
|---|---|
| Title | Experimental Studies on the Elastic-Plastic Behavior of Braced Frames under Repeated Horizontal Loading. Part 1 Experiments of Braces with an H-shaped Cross Section in a Frame |
| Author(s) | WAKABAYASHI, Minoru; NAKAMURA, Takeshi; YOSHIDA, Nozomu |
| Citation | Bulletin of the Disaster Prevention Research Institute (1977), 27(3): 121-154 |
| Issue Date | 1977-09 |
| URL | http://hdl.handle.net/2433/124870 |
| Right | |
| Type | Departmental Bulletin Paper |
| Textversion | publisher |

Kyoto University

# Experimental Studies on the Elastic-Plastic Behavior of Braced Frames under Repeated Horizontal Loading

### Part 1   Experiments of Braces with an H-shaped Cross Section in a Frame

Minoru WAKABAYASHI, Takeshi NAKAMURA
and Nozomu YOSHIDA

### Abstract

An experimental study is conducted to obtain the hysteretic characteristics of the brace itself in a braced frame under repeated loading. Braces with an H-shaped cross section are tested in a single or a double bracing system. The effects of the slenderness ratio, the buckling plane and the local buckling are investigated. Furthermore, the fundamental properties of a brace for the formulation of the hysteretic characteristics under repeated loading are extracted.

## 1.   Introduction

In Japan where earthquakes and windstorms are frequent, it is necessary for building structures to survive them. The vertical bracing system is widely used in practical design to give sufficient strength and rigidity under such external excitations. The load carrying capacity and the rigidity of braces under compression decreases rapidly after buckling. Under cyclic loading, the buckled brace behaves in an unstable manner and the shape of hysteresis loops are very complicated. In the design guide for high rise buildings[1], the use of braces with the slenderness ratio less than 40 is proposed to estimate simply the behavior of braces. In case of comparatively low rise buildings, the load carrying capacity of braces with fairly large slenderness ratio under compression used to be conventionally neglected. It is certified in the experimental studies[4] that the deterioration of the hysterstic characteristics of braces whose slenderness ratio is as small as 40 is pretty large under cyclic loading and that the compressive load carrying capacity of braces with rather large slenderness might be expected. Therefore it is essential to estimate reasonably the elastic-plastic hysteretic characteristics of braces under repeated loading in order to design braced structures appropriately.

In a dynamic response analysis of braced structures undergoing an earthquake, the formulated hysteretic characteristics of braces are required. In Japan, a number of studies on the hysteretic behavior of braces have been performed in the last ten

years. In the past studies, braces with a simple boundary condition such as simple support or rigidly fixed support were investigated[2]~[16]. General hysteretic rules under repeated axial loading have been obtained and it is recognized that the restoring-force characteristics of braces are strongly affected by the slenderness ratio. However, it is difficult to apply directly the hysteretic characteristics obtained from the studies of this kind to the response analysis of a braced frame. The process to derive the restoring force of braces is very complicated in the theoretical studies. Formulation of the behavior of braces has been hardly performed in experimental studies. Further-more, idealized members differ from actual braces in the following points: The rotation of the end of braces is restrained in an elastic or an elastic-plastic manner by a surrounding frame or a gusset plate etc. Braces are subjected to compulsory end deformation in the plane of a frame due to the story drift of a frame. Bracing members are frequently arranged intersecting each other, and hence they interact with each other. Such interaction behaviors between braces and the surrounding frame, and between the bracing members should be made clear.

Several experimental studies are conducted to obtain the hysteratic characteristics of one or two storied braced frame[17]~[25]. The behavior of braces themselves should be extracted from the whole behavior of the braced frame to apply the fruit of these experimental studies to more complicated systems which are actually used. However these examinations have not been performed in past studies.

The purpose of this research is to obtain the hysteretic characteristics of braces built in a frame under repeated loading, and to formulate them in order to apply directly to a dynamic response analysis of braced frames. The test results for braces with H-shaped cross section are reported in this paper. The report on the hysteretic characteristics of braces with other types of cross section; i. e. circular tube, angle, flat bar, and round bar braces, which are frequently used in actual design, the formulation of the hysteretic characteristics, and the response analysis using a formulated hysteretic rule will follow this paper.

## 2.  Test Plan

### 2.1  Planning of test

The experiment is conducted to obtain the hysteretic behavior of a steel brace put in a framed structure. Fig. 1 illustrates the typical types of bracing systems. The circled units in the figure are those tested. In order to obtain only the behavior of bracing members in a braced frame, a surrounding frame which does not resist any horizontal load is designed. Test parameters are as follows:

a)  Cross sectional shape

   Bracing members have an H-shaped cross section.

b)  Types of bracing

   Two of the most typical types used frequently in practical designs are tested, and they are illustrated in the circles of Fig. 1. They are referred to as single

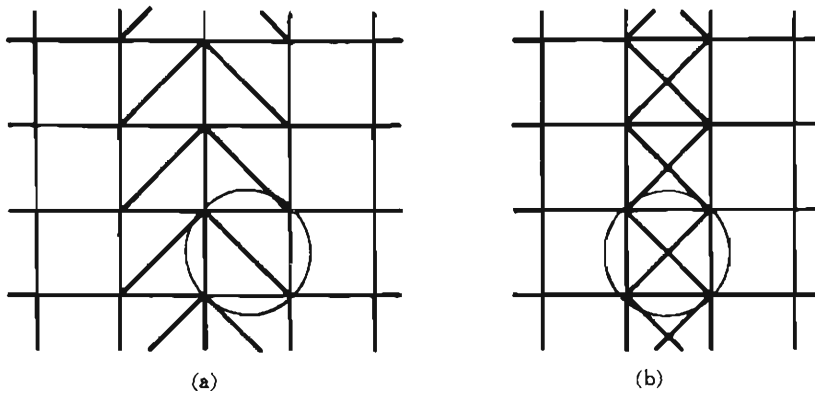(a)                                          (b)

Fig. 1.  Typical bracing systems.

and double bracing systems in this paper.

c)  Plane of buckling

The weak axis of a cross section is put in the plane of a frame or in the plane perpendicular to the plane of a frame. The former specimen buckles out of the plane of a frame and the latter buckles within the plane of a frame.

## 2.2  Test specimen

Each plate element of the specimen is cut out from the hot rolled steel plate of SS 41-grade with 6 mm thickness. The longitudinal direction of the cut plates coincides with the rolled direction. The plates are built up to H-shape by fillet welding with 2 mm leg length.  Dimensions of the H-shaped cross section are 50 mm in depth, 50 mm in width of flanges, and 6 mm in thickness of web and flanges (Built-up H-50×50×6×6). Built-up members are annealed under the thermal conditions shown in Fig. 2 to remove the residual stress due to welding. End plates are welded after annealing. Specimens are illustrated in Fig. 3. The ends of a specimen and the intersection of double bracing members are reinforced with steel plates as shown in the figure.
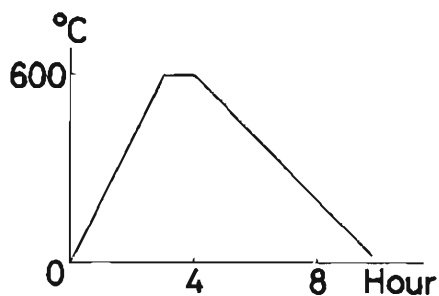


Fig. 2.  Thermal condition of annealing.

Mechanical properties of the used steel plate which are obtained from tension tests are shown in Table 1. Totally 24 specimens are tested. Measured dimensions and test parameters of each specimen are shown in Table 2.
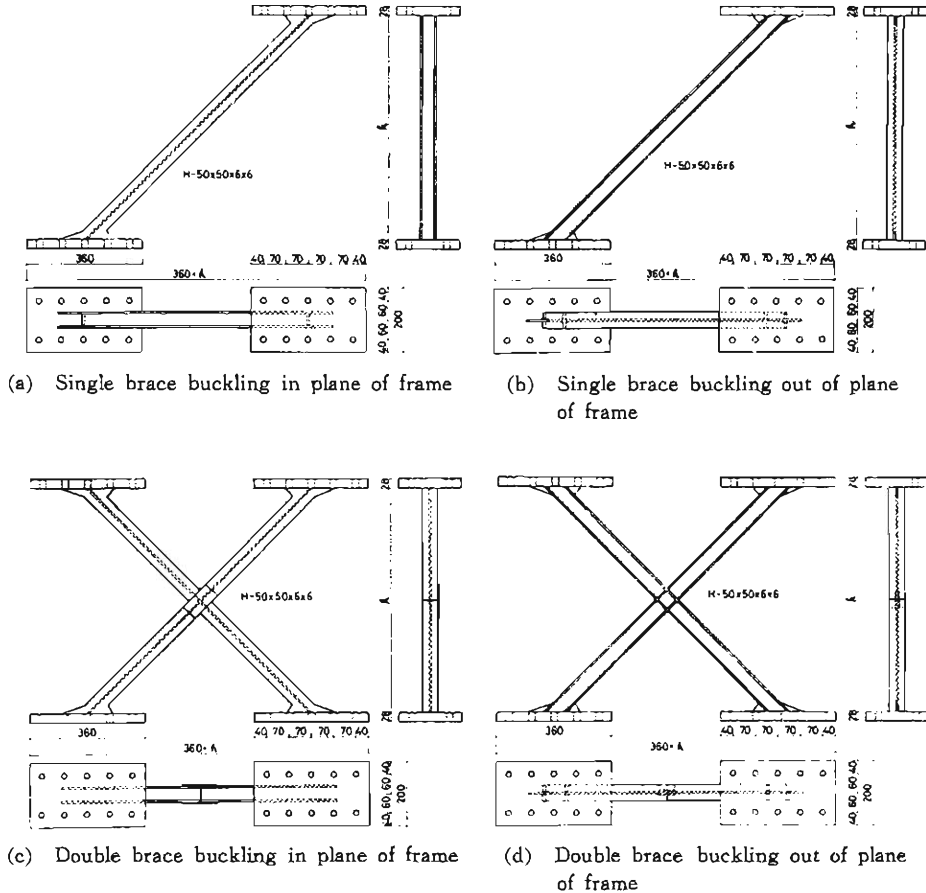


(a)  Single brace buckling in plane of frame

(b)  Single brace buckling out of plane of frame

(c)  Double brace buckling in plane of frame

(d)  Double brace buckling out of frame

Fig. 3.  Specimens

Table 1.  Mechanical properties of material

|  | Bar length is 1 and 2 m | Bar length is 3 m |
|---|---|---|
| Yield stress ($t/cm^2$) | 2.89 | 2.57 |
| Strain hardening strain ($\times 10^{-6}$) | 22000 | 27500 |
| Maximum stress ($t/cm^2$) | 4.38 | 3.77 |
| Ultimate strain | 0.383 | 0.409 |

Table 2. Test parameters and demension of the specimen[*1]

| Specimen[*2] name | Bracing system | Cross section and the plane of frame | Loading[*3] | $l$ (cm) | $B$ (cm) | $D$ (cm) | $t_w$ (cm) | $t_f$ (cm) | $A$ (cm²) | $\lambda$[*4] |
|---|---|---|---|---|---|---|---|---|---|---|
| SIM 1 | | | M | 98.46 | 5.05 | 5.03 | 0.592 | 0.631 | 8.60 | 39.1(24.9) |
| SIC 1 | | | C | 98.47 | 5.00 | 5.01 | 0.626 | 0.597 | 8.51 | 39.6(25.0) |
| SIM 2 | | I | M | 197.2 | 5.08 | 4.97 | 0.598 | 0.603 | 8.37 | 78.5(50.4) |
| SIC 2 | | | C | 197.0 | 5.05 | 5.04 | 0.602 | 4.598 | 8.37 | 79.1(49.7) |
| SIM 3 | | | M | 297.0 | 4.96 | 4.94 | 0.573 | 0.607 | 8.16 | 120.5(76.2) |
| SIC 3 | Single bracing | | C | 297.2 | 4.97 | 4.99 | 0.602 | 0.583 | 8.19 | 120.9(75.6) |
| SOM 1 | | | M | 99.00 | 5.11 | 5.07 | 0.613 | 0.602 | 8.52 | 39.4(24.8) |
| SOC 1 | | | C | 98.93 | 4.93 | 4.92 | 0.631 | 0.592 | 8.39 | 40.2(25.6) |
| SOM 2 | | | M | 196.8 | 5.02 | 4.96 | 0.593 | 0.603 | 8.28 | 79.2(50.4) |
| SOC 2 | | H | C | 197.0 | 5.04 | 4.94 | 0.614 | 0.603 | 8.43 | 78.8(50.8) |
| SOM 3 | | | M | 296.8 | 4.97 | 5.01 | 0.595 | 0.596 | 8.19 | 121.4(75.4) |
| SOC 3 | | | C | 296.8 | 5.00 | 5.01 | 0.597 | 0.596 | 8.24 | 120.5(75.3) |
| DIM 1 | | | M | 99.25 / 98.80 | 5.00 / 5.03 | 5.06 / 4.95 | 0.603 / 0.591 | 0.615 / 0.596 | 8.45 / 8.22 | 22.5(17.5) |
| DIC 1 | | | C | 98.82 / 98.78 | 4.99 / 5.02 | 5.07 / 4.95 | 0.621 / 0.604 | 0.599 / 0.600 | 8.49 / 8.31 | 22.4(17.4) |
| DIM 2 | | I | M | 198.0 / 197.3 | 5.03 / 5.07 | 4.94 / 5.02 | 0.598 / 0.593 | 0.606 / 0.624 | 8.48 / 8.56 | 44.2(35.6) |
| DIC 2 | | | C | 197.9 / 198.3 | 5.07 / 4.99 | 4.95 / 5.19 | 0.604 / 0.606 | 0.594 / 0.593 | 8.34 / 8.41 | 44.1(35.5) |
| DIM 3 | | | M | 296.5 / 296.0 | 5.00 / 4.98 | 5.05 / 4.99 | 0.597 / 0.590 | 0.607 / 0.605 | 8.35 / 8.25 | 67.4(52.2) |
| DIC 3 | Double bracing | | C | 296.8 / 296.4 | 4.97 / 4.96 | 5.01 / 4.93 | 0.604 / 0.599 | 0.585 / 0.598 | 8.23 / 8.17 | 67.7(52.7) |
| DOM1 | | | M | 98.71 / 99.04 | 5.04 / 4.93 | 5.04 / 5.04 | 0.604 / 0.590 | 0.595 / 0.605 | 8.32 / 8.23 | 27.9(14.0) |
| DOC 1 | | | C | 99.20 / 99.30 | 5.01 / 5.07 | 4.97 / 5.03 | 0.596 / 0.609 | 0.601 / 0.601 | 8.24 / 8.46 | 28.1(14.2) |
| DOM2 | | | M | 198.2 / 198.0 | 5.03 / 5.04 | 5.02 / 5.07 | 0.595 / 0.598 | 0.609 / 0.621 | 8.38 / 8.58 | 55.7(28.0) |
| DOC 2 | | H | C | 197.8 / 198.2 | 5.02 / 5.09 | 4.93 / 5.03 | 0.611 / 0.611 | 0.610 / 0.602 | 8.34 / 8.51 | 55.7(28.6) |
| DOM3 | | | M | 296.5 / 297.0 | 4.98 / 4.99 | 4.99 / 4.99 | 0.600 / 0.577 | 0.607 / 0.604 | 8.17 / 8.20 | 84.4(42.1) |
| DOC 3 | | | C | 297.3 / 296.9 | 4.99 / 5.00 | 5.00 / 4.99 | 0.598 / 0.587 | 0.580 / 0.578 | 8.17 / 8.07 | 84.3(42.3) |

*1  The quantities of compression and tension member of a double brace are shown in the upper and lower line.

*2  Each letter of specimen name represents test parameters, i. e..

    $S$ : single bracing system,    $D$ : double bracing system,

    $I$ : in plane buckling,    $O$ : out of plane buckling,

    $M$ : monotonic loading,    $C$ : cyclic loading,

    1, 2, 3 : length of specimen (unit; meter).

*3  $M$ : monotonic Loading, $C$ : Cyclic Loading.

*4  ( ) : effective slenderness ratio about strong axis of cross section.

## 2.3  Test set-up and measurement

Figure 4 shows the test set-up schematically, and the whole view of the test is shown in Photo 1. The test set-up is composed of a loading frame, a 50 ton push-pull type hydraulic jack and two load cells, and supporting blocks. The loading frame does not resist any horizontal load because the beam and the column are connected by a pin at each joint. The supporting blocks sustain the reaction of horizontal forces. They are fixed to a reaction floor by high strength steel bolts with 33 mm diameter. The loading frame can move freely in the plane of a frame, but out-of-
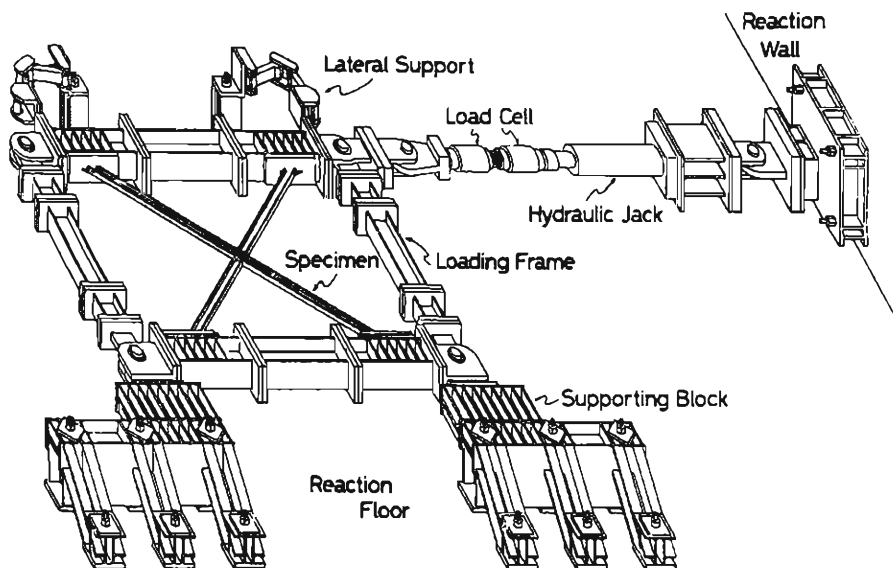


Fig. 4.  Test set-up
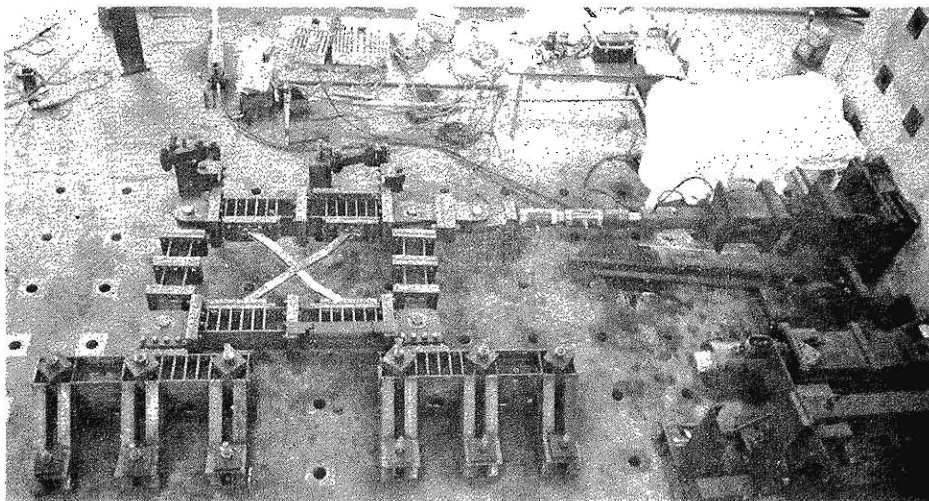


Photo 1.  Whole view of test.
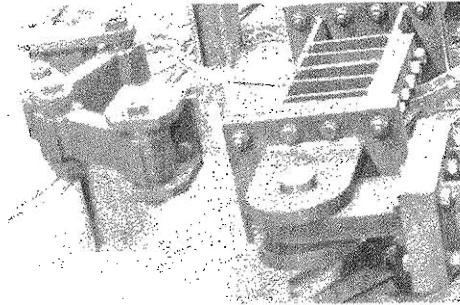
Photo 2. Lateral support.

plane movement is prevented by two lateral supports (Photo 2).

The horizontal load is measured by load cells. The relative horizontal displacement between the upper and the lower beams of the loading frame is measured by a dial gage. The axial deformation of a bracing member are measured by a potentio meter. The lateral deflections about two major axes of a cross section and the torsional deformation are measured by three potentio meters. Four pieces of strain gage to a section are mounted at several portions along the longitudinal direction of braces to measure bi-axial bending stress and longitudinal stress.

## 2.4 Loading program

Twelve specimens are subjected to monotonic load and 12 specimens are subjected to cyclic load. The loading in cyclic test is controlled on the basis of the amplitude of the story drift angle. The programmed story drift angle versus the number of cycle of loading relation is shown in Fig. 5.
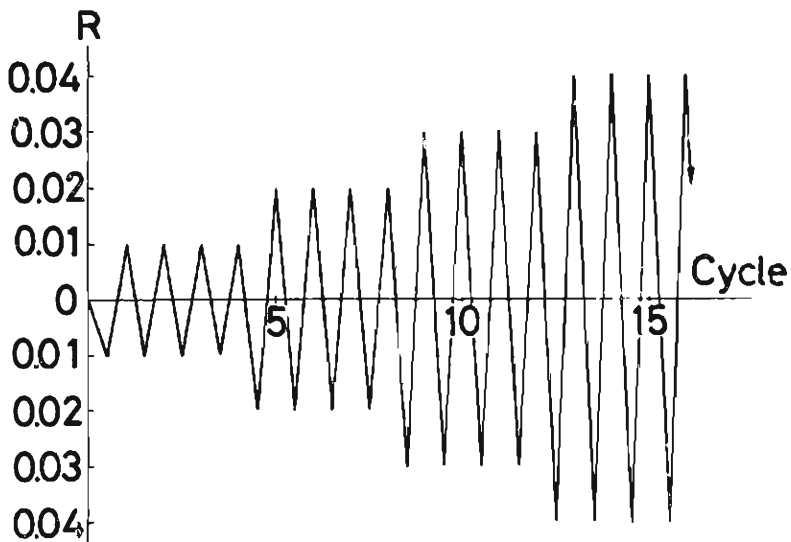


Fig. 5. Loading program.

The stabilization of hysteresis loops is observed in four cycles of loading in each displacement amplitude.

## 2.5  Setting of the specimen to the loading frame

The initial deflection are measured before the specimens are fixed to the loading frame. Initial deflections along the tip edge of the flange are substituted for that of the center of gravity of a cross section, which can not be measured directly. Fig. 6 shows examples of measured initial deflection, and the maximum value of the initial deflection of each specimen is shown in Table 3.

High tensile bolts are used to connect the end plates of the specimen to the beams of the loading frame. Though steel plates with various thickness are inserted between the end plate and the beam not to induce initial stress to the specimen, some initial stress is induced inavoidably, and its magnitude generally depends on
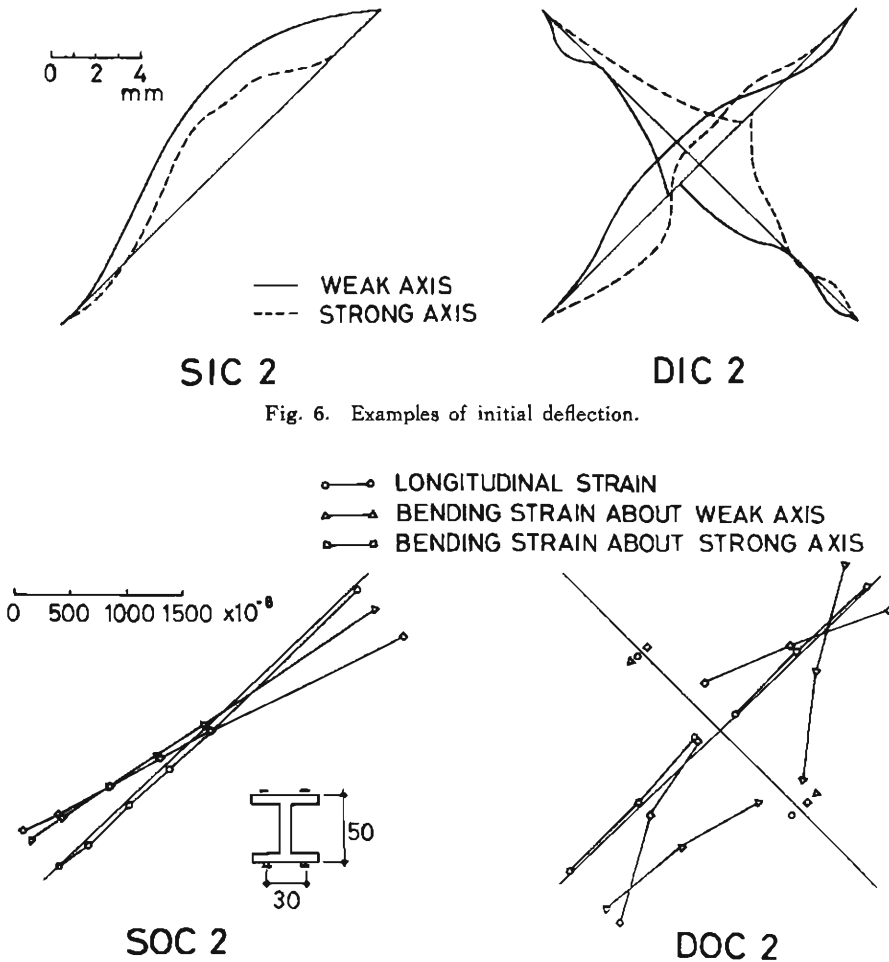


Fig. 6.  Examples of initial deflection.



Fig. 7.  Examples of initial strain.

Table 3. Results of test

| Specimen name | Maximum initial deflection (mm) strong axis | work axis | Maximum measured initial strain ($\times 10^{-6}$) | Buckilng Load (ton) | Number of cycle when Local buckling is observed | Number of cycle when crack is observed | Remarks |
|---|---|---|---|---|---|---|---|
| SIM 1 | 0.16 | 0.00 | 453 | 16.98 | — | — | |
| SIC 1 | 1.35 | 1.72 | 525 | 17.90 | 9 | 10 | |
| SIM 2 | — | — | 411 | 11.63 | — | — | |
| SIC 2 | 3.00 | 2.10 | 569 | 11.98 | — | 13 | |
| SIM 3 | 3.18 | 1.20 | 283 | 7.65 | — | — | |
| SIC 3 | 0.99 | 4.25 | 150 | 7.90 | — | — | |
| SOM 1 | 0.39 | 0.89 | 651 | 17.54 | — | — | |
| SOC 1 | 0.96 | 1.30 | 540 | 16.98 | 5 | — | |
| SOM 2 | 1.00 | 1.40 | 417 | 11.04 | — | — | |
| SOC 2 | 1.60 | 1.00 | 407 | 12.45 | — | — | |
| SOM 3 | 1.44 | 2.07 | 220 | 7.14 | — | — | |
| SOC 3 | — | — | 322 | 7.05 | — | — | |
| DIM 1 | 0.46 0.89 | 1.13 1.00 | 932 | 33.49 | — | — | |
| DIC 1 | 1.65 3.38 | 0.90 0.87 | 774 | 35.55 | 5 | 8 | |
| DIM 2 | — | — | 324 | 32.14 | — | — | |
| DIC 2 | 2.26 1.62 | 1.33 2.85 | 627 | 32.48 | — | 6 | |
| DIM 3 | 2.47 — | 2.23 | 205 | 24.71 | — | — | |
| DIC 3 | 3.41 5.02 | 2.55 2.03 | 338 | 27.15 | — | 9 | |
| DOM1 | 0.51 0.80 | 0.63 1.22 | 920 | 36.86 | — | — | |
| DOC 1 | 1.92 0.87 | 1.44 2.47 | 778 | 37.0 | 6 | 13 | |
| DOM2 | — | — | 654 | 30.78 | — | — | |
| DOC 2 | 2.65 5.10 | 1.87 2.70 | 900 | 32.88 | 13 | 14 | |
| DOM3 | 3.94 — | 3.10 — | 393 | 25.11 | — | — | |
| DOC 3 | — | — | 316 | 23.45 | — | — | |

the rotation of the end plates, judging from the measured strains. Some examples of the distribution of initial stress induced before loading are shown in Fig. 7, and the maximum values of strains measured after setting are shown in Table 3.

## 3. Hysteretic behavior of braces obtained from experiment

### 3.1 General behavior of braces

There are several fundamental rules on the behavior of braces, which are understood from simple concepts in mechanics. The behavior of braces is generalized as follows, based on the fundamental rules.

(a)  The behavior of single braces

The behavior of a single brace is illustrated schematically in Fig. 8. Figs. 8(a) and 8(b) represent the horizontal load-horizontal displacement relation and the horizontal load-midpoint lateral deflection about a weak axis of a cross section relation, respectively. The idealized deflected shape based on the theoretical analysis are also shown in the figure. The marks ● and ○ on the deflected shapes in the figure represent that the cross section of the bar is yielding under the combined action of compression force and bending moment, and tensile force and bending moment, respectively, and ----- shows that the bar is yielding in pure tension.

The hysteretic curve is almost linear in the virgin elastic state although the specimen has initial imperfections such as initial stress and initial deflection. The maximum load carrying capacity is reached at point ①. After that, the sustained load of the monotonically loaded specimen decreases monotonically, and the slope of the falling branch decreases as the deformation increases. The bar is plastified near the ends and the mid-length of the bar under the combined action of compression force and bending moment.
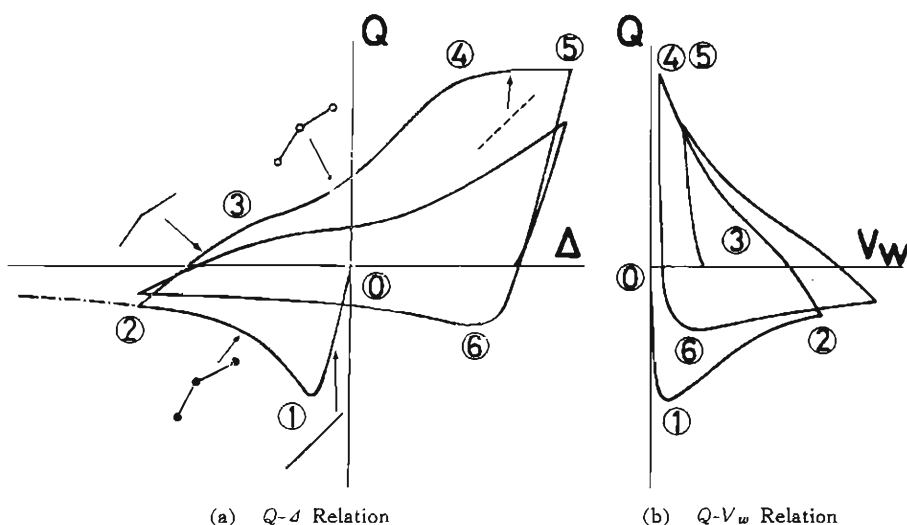


(a)  $Q$-$\varDelta$ Relation          (b)  $Q$-$V_w$ Relation

Fig. 8.  Schematic behavior of single brace

The loading direction is reversed at the prescribed point ②. The slope of *Q-Δ* curve at the elastic recovery range is much smaller than that in the initial elastic state due to the existence of the lateral deflection. The bar yields near point ③ under the combined action of tensile force and bending moment, and the slope once decreases. However, it increases again as the lateral deflection decreases. The horizontal load comes to the yield value at point ④, and the yield plateau appears between points ④ and ⑤. Though the lateral deflection does not disappear and the shape of the bar is not perfectly straight, the bar might be considered to be yielding in pure tension. The bar puts forth the maximum compression load carrying capacity at point ⑥ in the second cycle of loading. The horizontal load at point ⑥ is much smaller than the maximum load carrying capacity in the first cycle of loading, because of the existence of residual lateral deflection and Bauschinger's effect etc. Since the bar is stretched plastically in the first cycle of loading, the lateral deflection in the second cycle of loading is larger than that in the first cycle.

The behavior in the third and fourth cycles of loading is quite similar to the one in the second cycle, but the maximum tension and compression load carrying capacity becomes smaller because the bar length becomes longer as the number of loading cycles becomes larger. Hysteretic loops in each displacement amplitude are similar to each other, however, the maximum load carrying capacity becomes smaller as the displacement amplitude becomes larger.

The lateral deflection about the strong axis of a cross section and the torsional deformation are scarcely observed in the whole process of loading.

(b)   The behavior of double braces

The horizontal load-horizontal displacement relation and the idealized deflected
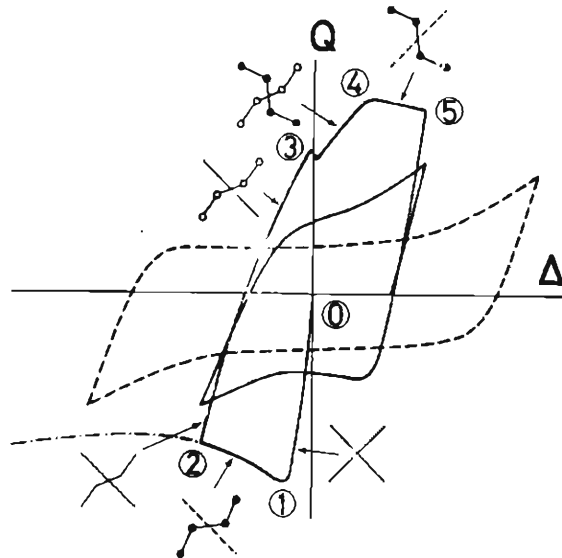


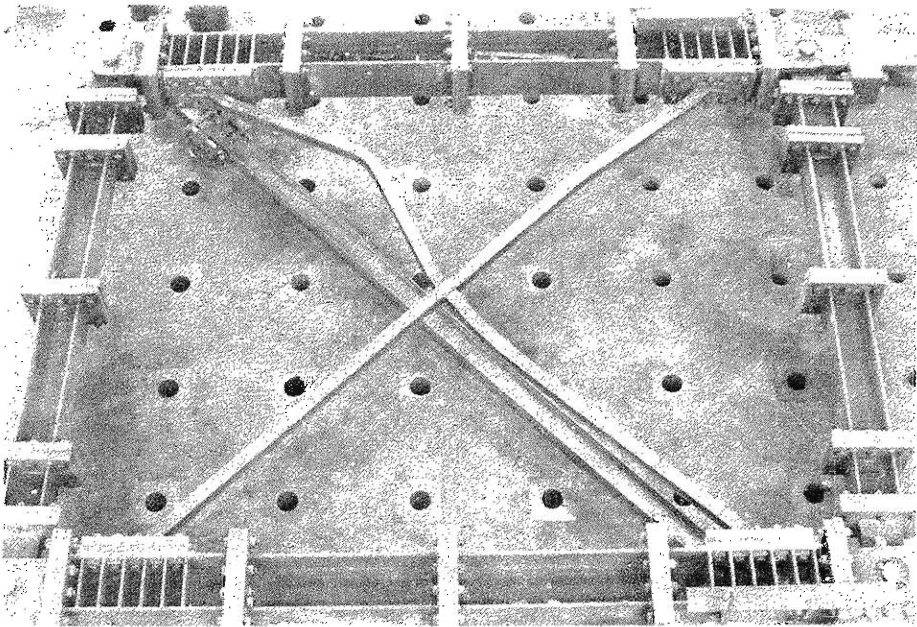Fig. 9. Schematic behavior of double brace

Photo 3.   Unsymmetrically deflected shape.

shapes of a double brace are illustrated in Fig. 9. The hysteretic curve at the virgin
state is almost linear in spite of the existence of initial imperfections.  The deflected
shape is symmetric about the intersection of both members when the compression
member buckles near point ①. However, it becomes unsymmetric (Photo 3) after
several cycles of loading, because the bending deformation of the member under
alternately repeated loading concentrates in a half side divided by the tension mem-
ber and the other half gradually becomes straight as a loading cycle increases.  The
deflected shape of braces with large slenderness ratio becomes unsymmetric more
easily than the ones with small slenderness ratio.

After the maximum load carrying capacity is reached, the sustained load decreases
because of the combined action of the post buckling behavior of the compression
member and the post yielding behavior of the tension member. In the monotonic
loading test, the sustained load increases again in the large deformation range, since
strain hardening in the tension member compensate for the decrease of the load
carrying capacity of the compression member.

Loading direction is reversed at point ② in the cyclic loading test, and the
specimen comes back to the elastic state. Until the tension member yields in pure
tension (Point ④), the tensile member yields under the combined action of tensile
force and bending moment, and the compression member buckles. In case of the
bar with large slenderness ratio, buckling of the compression member can be ob-
served clearly in the sudden decrease of the sustained load (Point ③). Points ③
and ④ are very close if the bar length is rather short, and they can not be distin-
guished. Since, between points ④ and ⑤, the tensile member yields in pure tension

and the compression member is under post-buckling state, the sustained load de-creases gradually.

After the second cycle of loading in each displacement amplitude, the sustained load deteriorates as a loading cycle increases, mainly because of the cumulated plastic elongation. The hysteretic loop has generally a fat reversed S-shape contain-ing hardening ranges and slip ranges. The load carrying capacity in the slip range is affected by the slenderness ratio.

The lateral deflection in the out-of-plane direction and the torsional deformation are scarcely observed when the specimen buckles and deflects within the plane of a frame. On the other hand, when the specimen buckles out of the plane of a frame, fairly large torsional deformation is observed in the tension member according to the out-of-plane deformation of the compression member.

In the cyclic loading test, local buckling takes place in the flange elements after
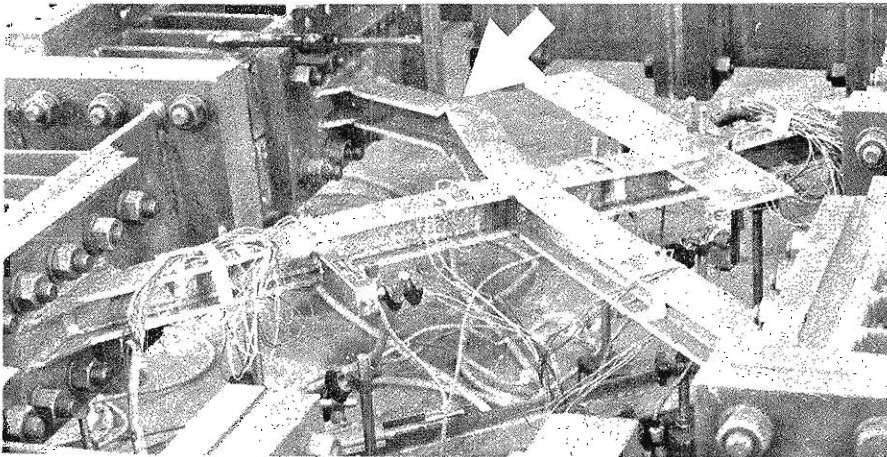


Photo 4. (a)　Concentration of bending deformation.
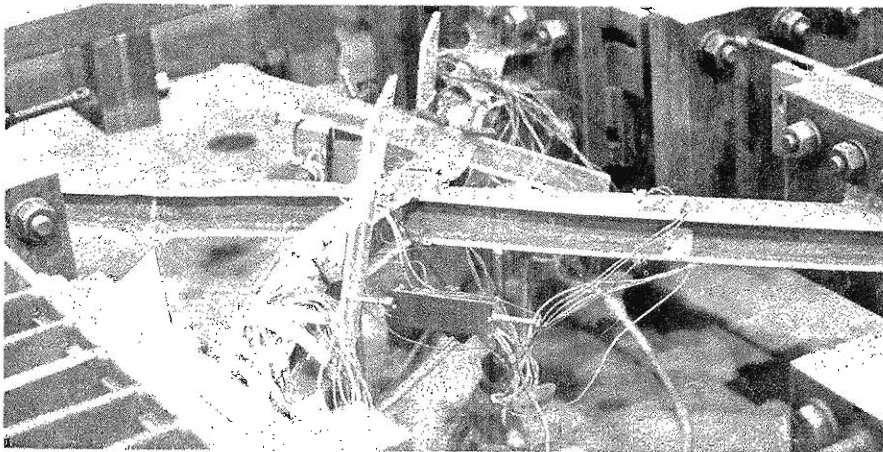


Photo 4. (b)　Cracks at locally buckled portion.

several cycles of loading. No remarkable change is observed on the $q$-$\delta$ curve when local buckling occurs. Plastic bending deformation concentrates at the locally buckled portions in subsequent loading (Photo 4(a)). The flange at these portions are subjected to large alternately repeated plastic deformation and cracks take place (Photo 4(b)). At last, the breakage of the bar is initiated at the cracked portion.

### 3.2 Behavior of each brace

The horizontal load-horizontal displacement relations obtained from the test are shown in Figs. 10-23. Figs. 10 and 11 are the results of the monotonic loading test and Figs. 12-23 are the results of the cyclic loading test. Axial force and axial displacement of single bracing members are derived from the equilibrium and the compatibility equations, i. e.

$$N_A = \sqrt{2}\ Q \qquad\qquad (1)$$
$$\Delta_A = \Delta/\sqrt{2} \qquad\qquad (2)$$

In case of double bracing, $N_A$ represents the sum total of axial forces in the tension and the compression members. The horizontal displacement-axial displacement relation obtained from the test satisfies Eq. (2) in fact. The results of each specimen are summarized in Table 3. Almost all specimens buckle and deflect about the weak axis of a cross section, whose general behavior has been explained in the former sections. However, a few specimens buckle about the strong axis of a cross section, and they have fairly different hysteretic characteristics compared with the other specimens.
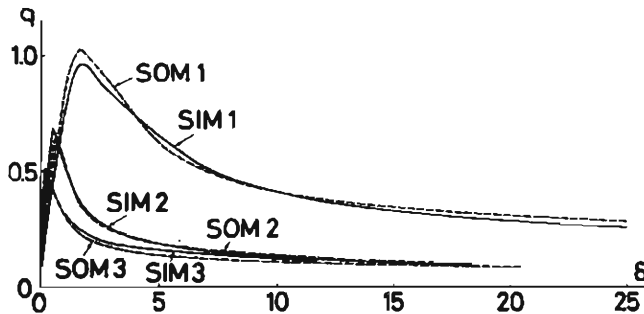


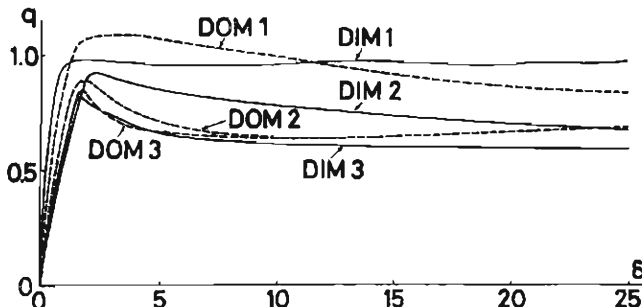Fig. 10.   $q$-$\delta$ relation of monotonically loaded single brace.



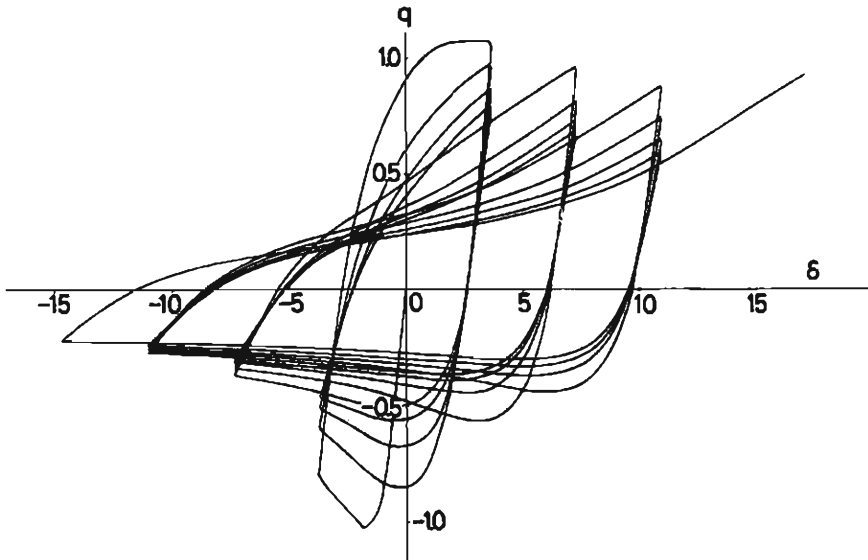Fig. 11.   $q$-$\delta$ relation of monotonically loaded double brace.
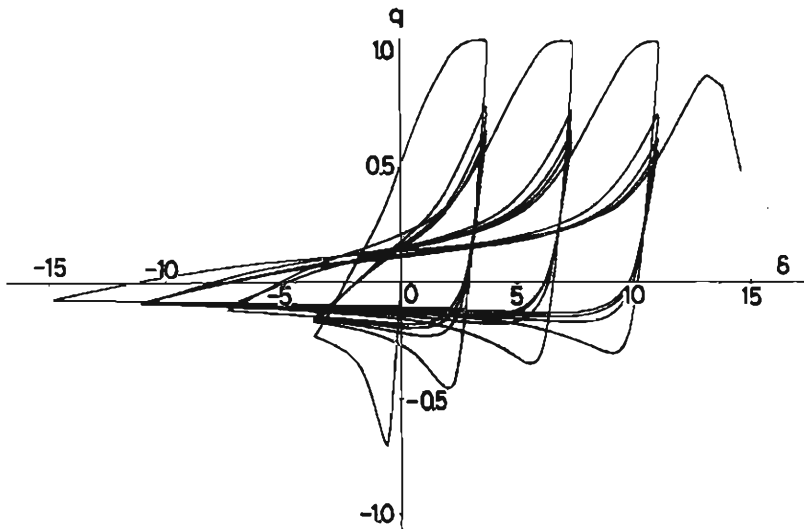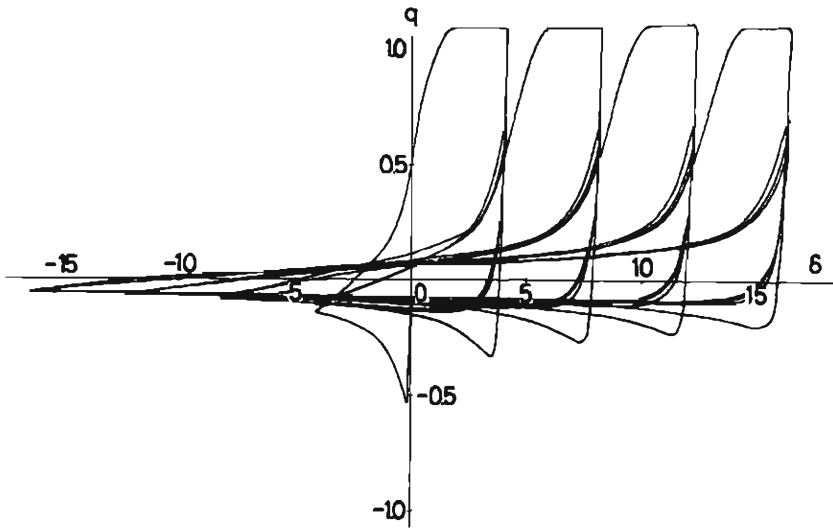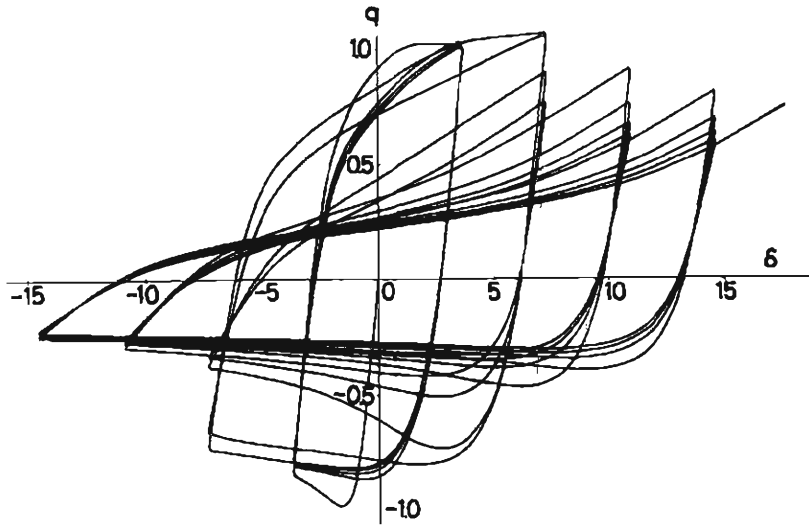
Fig. 12.   $q$-$\delta$ relation of *SIC* 1.



Fig. 13.   $q$-$\delta$ relation of *SIC* 2.

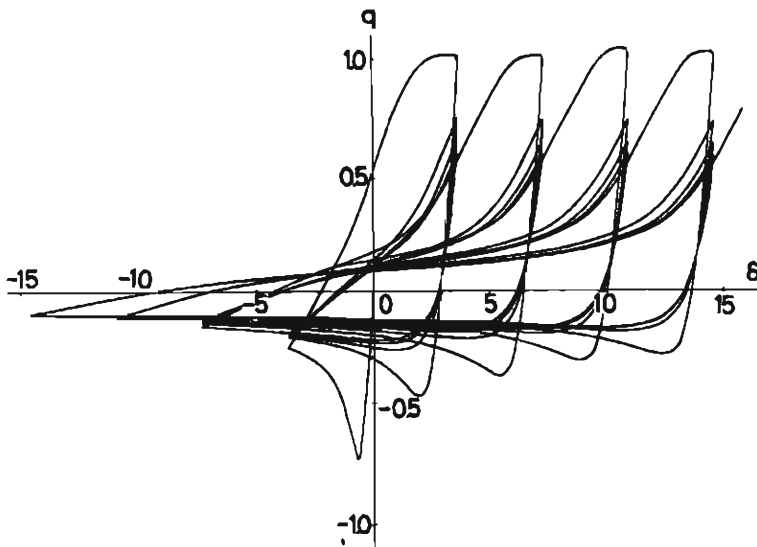Fig. 14.   $q$-$\delta$ relation of *SIC* 3.



Fig. 15.   $q$-$\delta$ relation of *SOC* 1.

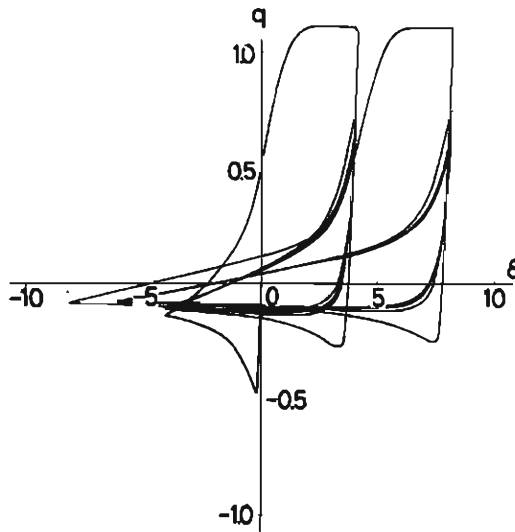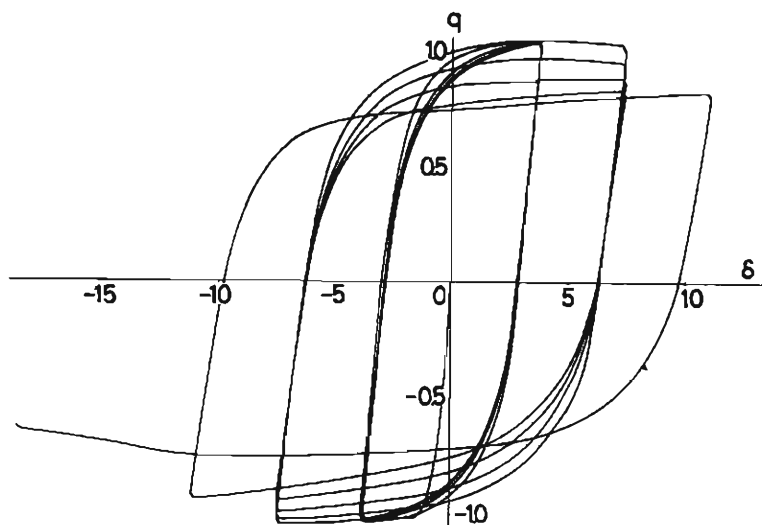Fig. 16. $q$-$\delta$ relation of *SOC* 2.
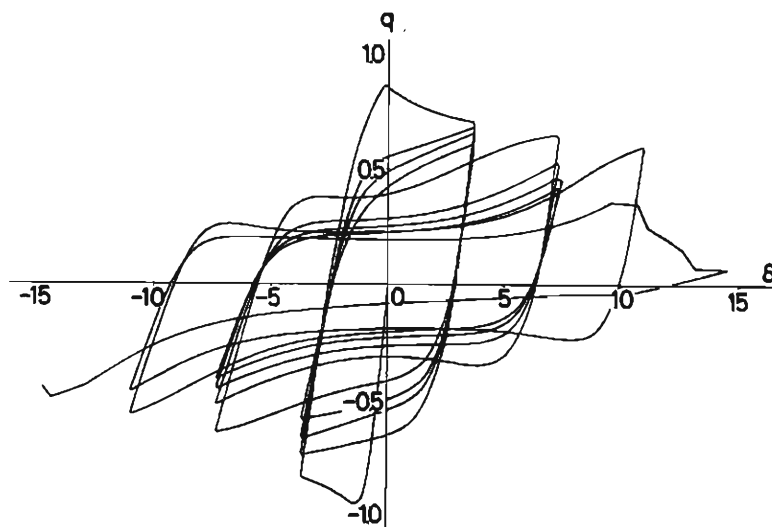


Fig. 17. $q$-$\delta$ relation of *SOC* 3.

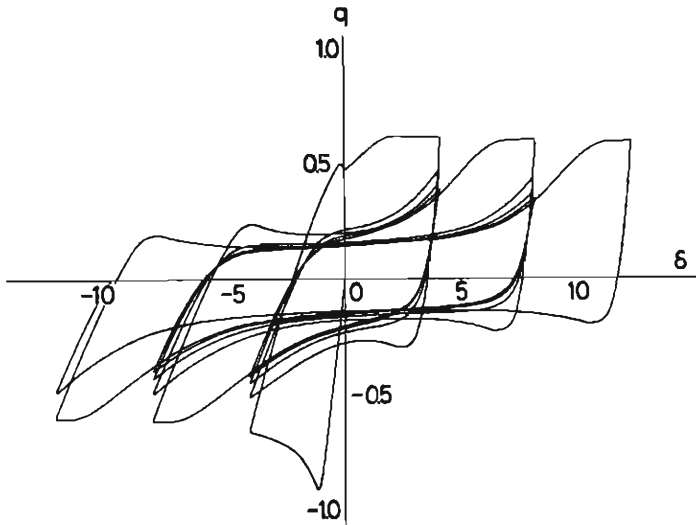Fig. 18.   $q$-$\delta$ relation of *DIC* 1.



Fig. 19.   $q$-$\delta$ relation of *DIC* 2.

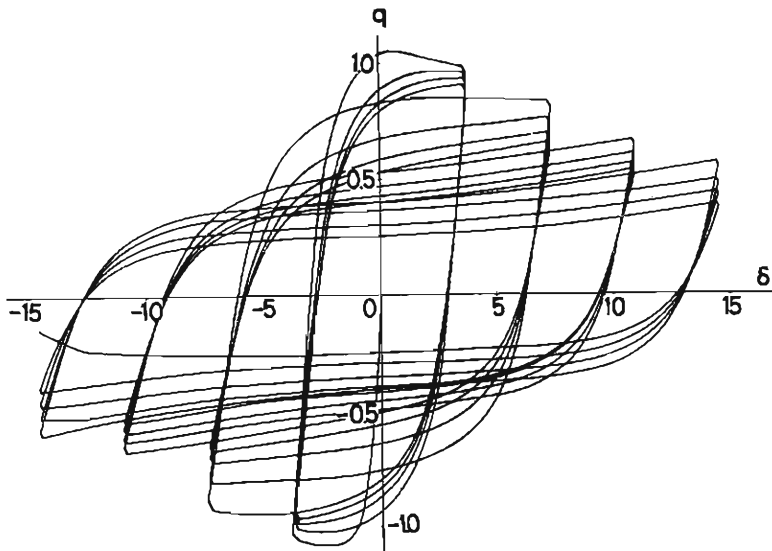Fig. 20. $q$-$\delta$ relation of *DIC* 3.
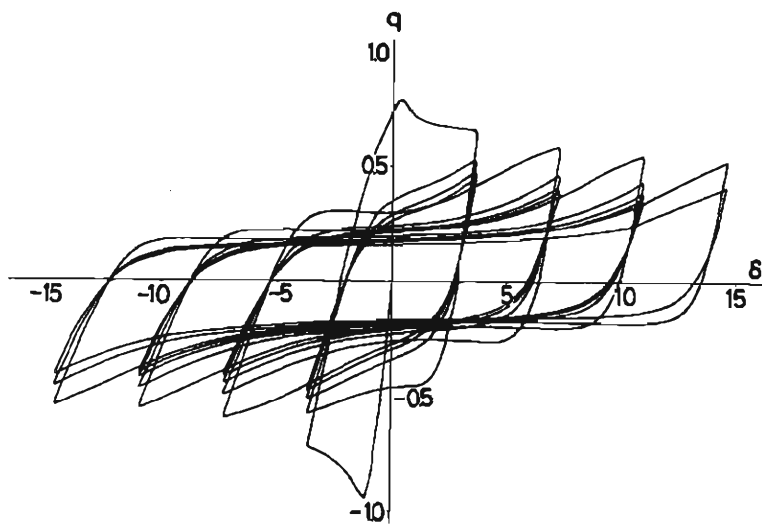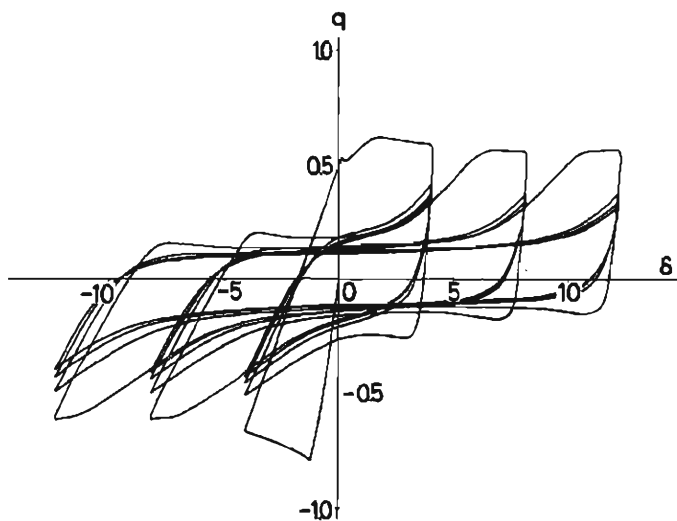


Fig. 21. $q$-$\delta$ relation of *DOC* 1.

Fig. 22.   $q$-$\delta$ relation of *DOC* 2.



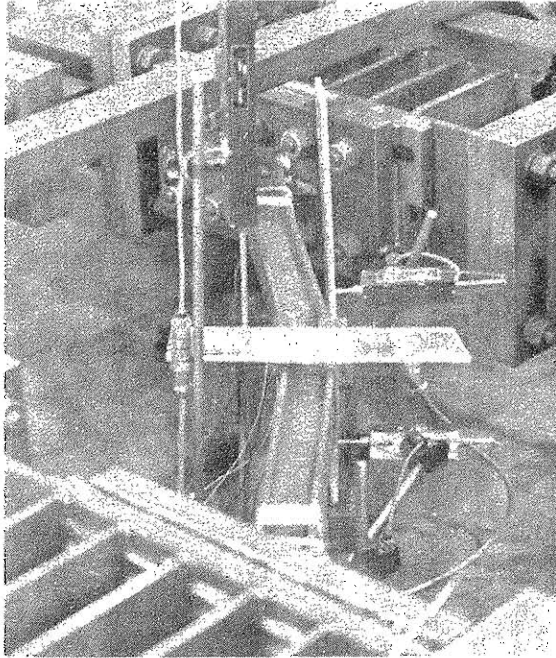Fig. 23.   $q$-$\delta$ relation of *DOC* 3.

Photo 5   Deformation of *SOC* 1 about strong axis of
cross section.

The specimen named *SOC* 1 (single brace which is designed to buckle out of plane of a frame and the slenderness ratio of which is 40. 2) buckles about the strong axis of a cross section (Photo 5). The effective slenderness ratio about strong axis of a cross section is 25. 6. The lateral deflection about weak axis of a cross section is small until the sixth cycle of loading, and the specimen shows stable hysteretic characteristics, i. e. the deterioration of the load carrying capacity is very small. However, in the seventh cycle of loading, the lateral deflection about weak axis of a cross section suddenly becomes large and the sustained load decreases rapidly. In the subsequent stage, the lateral deflection about the weak axis becomes predominant and that about strong axis disappears, and the hysteretic loop becomes a similar shape to *SIC* 1 which has the same length and buckles originally about the weak axis of a cross section. The transition of deflection at the mid-length is shown in Fig. 24.

In case of the specimen named *DIC* 1 (double brace which is designed to buckle within the plane of a frame, and the slenderness ratio of which is 22. 4), a half part of the compression member buckles about the weak axis and the other part buckles about the strong axis of a cross section at a virgin loading. The effective slenderness ratio about strong axis buckling is 17. 4. A stable, spindle-shape hysteretic loop is obtained until the lateral deflection about the weak axis becomes predominant at the sixth cycle of loading.
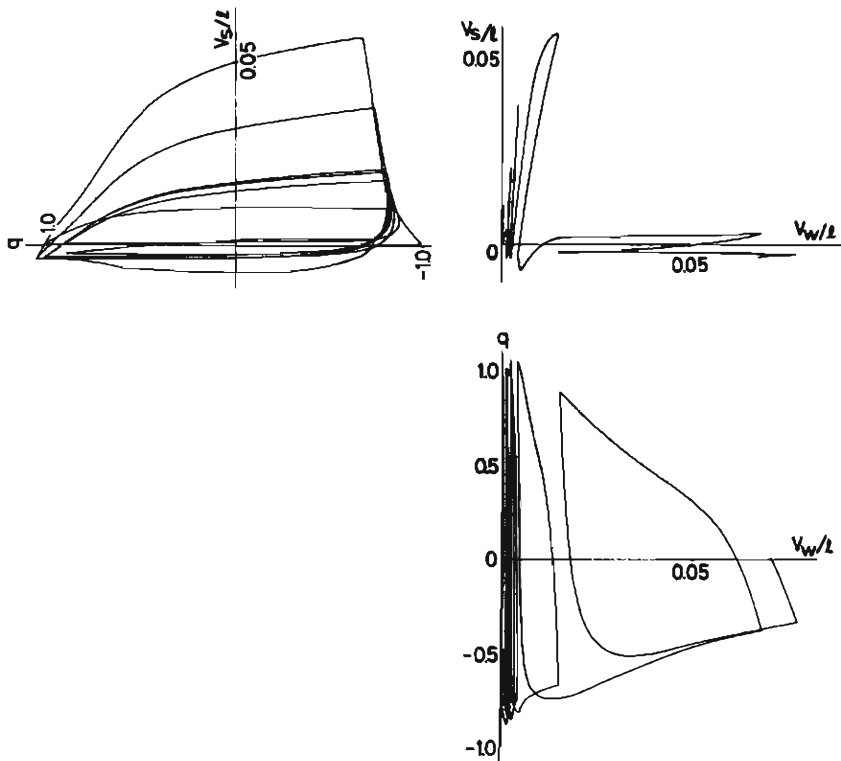
Fig. 24.   Translation of deflection of SOC 1.

## 4.   Considerations on the test results

### 4.1   Effective slenderness ratio

The boundary conditions at the ends of the bracing member are considered to be clamped because the flexural rigidity of the beams of the loading frame and the end plates is quite higher than that of the bracing members. Therefore the effective length of the single brace for buckling is a half of the bar length. The effective slenderness ratio is represented by

$$\lambda = l/2\, i, \qquad\qquad\qquad (3)$$

where $l$ denotes the bar length and $i$ denotes the radius of gyration of area.

The effective slenderness ratio of the double brace is calculated from the elastic buckling load derived from the slope-deflection method which takes into account the secondary effect of axial load. A double brace is modelized as shown in Fig. 25(a). Six independent deformations (three displacements and three rotations at the intersection) are shown in Fig. 25(b). Six equations are derived from the slope-deflection method.
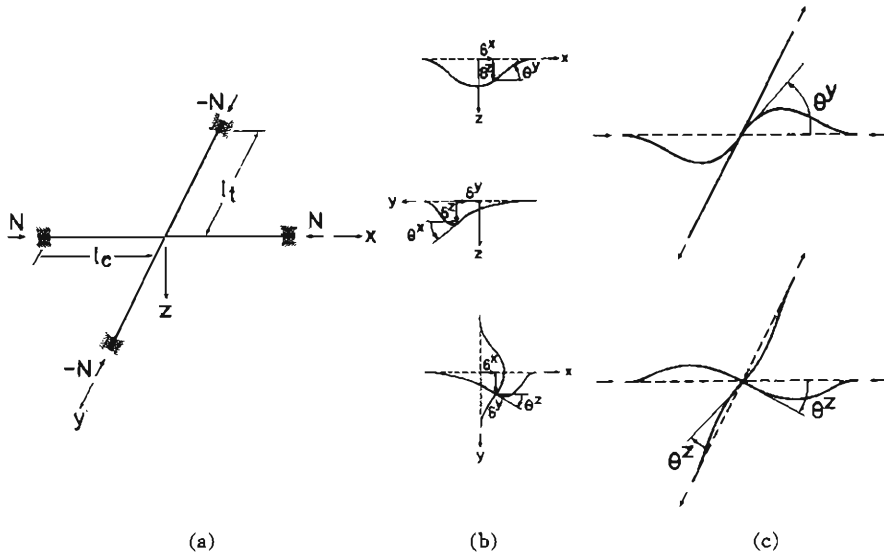
Fig. 25. (a) Buckling model of double brace
(b) Independent displacements
(c) Buckling mode

$$\alpha_t^x \theta^x = 0 \tag{4 a}$$

$$\alpha_t^x \theta^y = 0 \tag{4 b}$$

$$(I_c^z \, \alpha_c^z / l_c + I_t^z \, \alpha_t^z / l_t) \theta^z = 0 \tag{4 c}$$

$$(2 \, \gamma_t^z - N l_t^2 / E I_t^x) \delta^x = 0 \tag{4 d}$$

$$(2 \, \gamma_c^z - N l_c^2 / E I_c^y) \delta^y = 0 \tag{4 e}$$

$$\left( \frac{I_c^y}{l_c^2} \gamma_c^y - \frac{I_t^x}{l_t^2} \gamma_t^z \right) \delta^z = 0 \tag{4 f}$$

where the subscript $c$ and $t$ denote the quantities about a compression and a tension member, respectively, and the superscript $x$, $y$ and $z$ denote the corresponding axis. $I$ is the moment of inertia. $E$ is Young's modulus. $l$ is a half length of a brace, and

$$\alpha = \frac{Z \sin Z - Z^2 \cos Z}{2(1 - \cos Z) - Z \sin Z}$$

$$\gamma = \frac{Z^2 \cos Z - Z^2}{2(1 - \cos Z) - Z \sin Z}$$

$$Z^2 = N l^2 / E I$$

where $N$ is taken positive in compression. The coefficient of Eq. (4c) is equal to zero for in-plane buckling, and that of Eq. (4b) is zero for out-of-plane buckling. The corresponding buckling mode is shown in Fig. 25(c). The effective slenderness ratio is represented as

$$\lambda = \pi \sqrt{EA/N_B} \qquad\qquad\qquad (5)$$

where $N_B$ is the elastic buckling load and $A$ is the cross sectional area. Calculated effective slenderness ratio is shown in Table 2.

When the torsional rigidity of members is taken into account, the coefficients of Eqs. (4a) and (4b) are changed slightly. However, elastic buckling loads are hardly changed, as the comparison between the results of two kinds of analyses is shown in Table 4. The buckling stress-effective slenderness ratio relation is shown in Fig. 26. Solid and hollow circles denote a single and a double brace, respectively. Solid line denotes Euler's formula and dashed line denotes the yield stress. Chain line denotes the parabolic approximation curve in inelastic range (Eq. (6)) based on the AIJ design standard for steel structures.

$$\sigma_{cr} = \{1 - 0.4(\lambda/\sqrt{\pi^2 \overline{E}/0.\overline{6}\,\overline{\sigma}_y})^2\}\sigma_y \qquad\qquad (6)$$

Judging from Fig. 26, estimation of the effective slenderness ratio is sufficiently reasonable.

The effective slenderness ratio of the double brace for buckling and for the behavior under repeated loading should be essentially different, because of the following reasons :

Table 4.  Comparison of buckling load*.

| Bar length(m) | Buckling load when torsional rigidity is considered (ton) | Buckling load when torsional rigidity is neglected (ton) | Difference |
|---|---|---|---|
| 1 | 218. 48 | 217. 51 | 0. 0041 |
| 2 | 54. 44 | 54. 38 | 0. 0011 |
| 3 | 24. 18 | 24. 17 | 0. 0017 |

*1  Nominal dimensions are used in the calculation



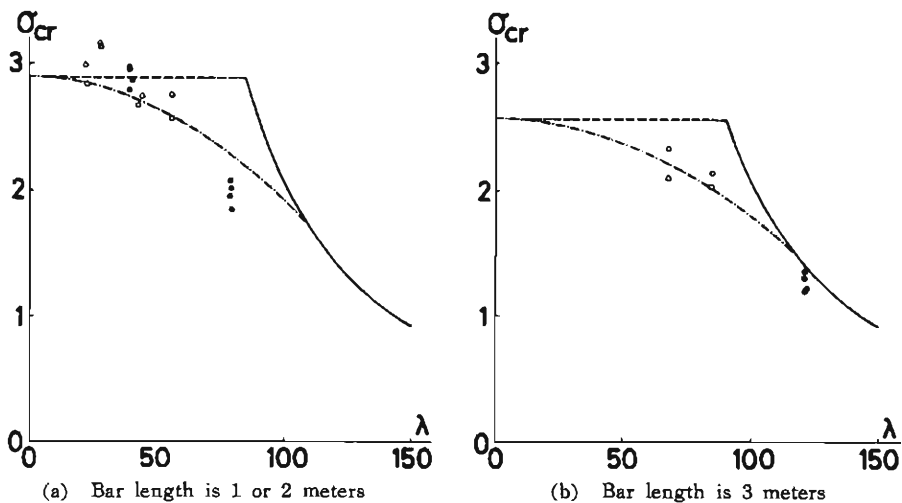(a)  Bar length is 1 or 2 meters      (b)  Bar length is 3 meters
Fig. 26.  Buckling stress-effective slenderness ratio relation.

1° The stress distribution and the distance between inflection points under repeated loading differ from those at the instance of buckling because of the plastification due to the lateral deflection.

2° Deflected shape changes from symmetric to unsymmetric during repeated loading.

3° Restraining effect at the mid-joint for one member by another member is changed due to plastification.

## 4.2 Deterioration of the load carrying capacity

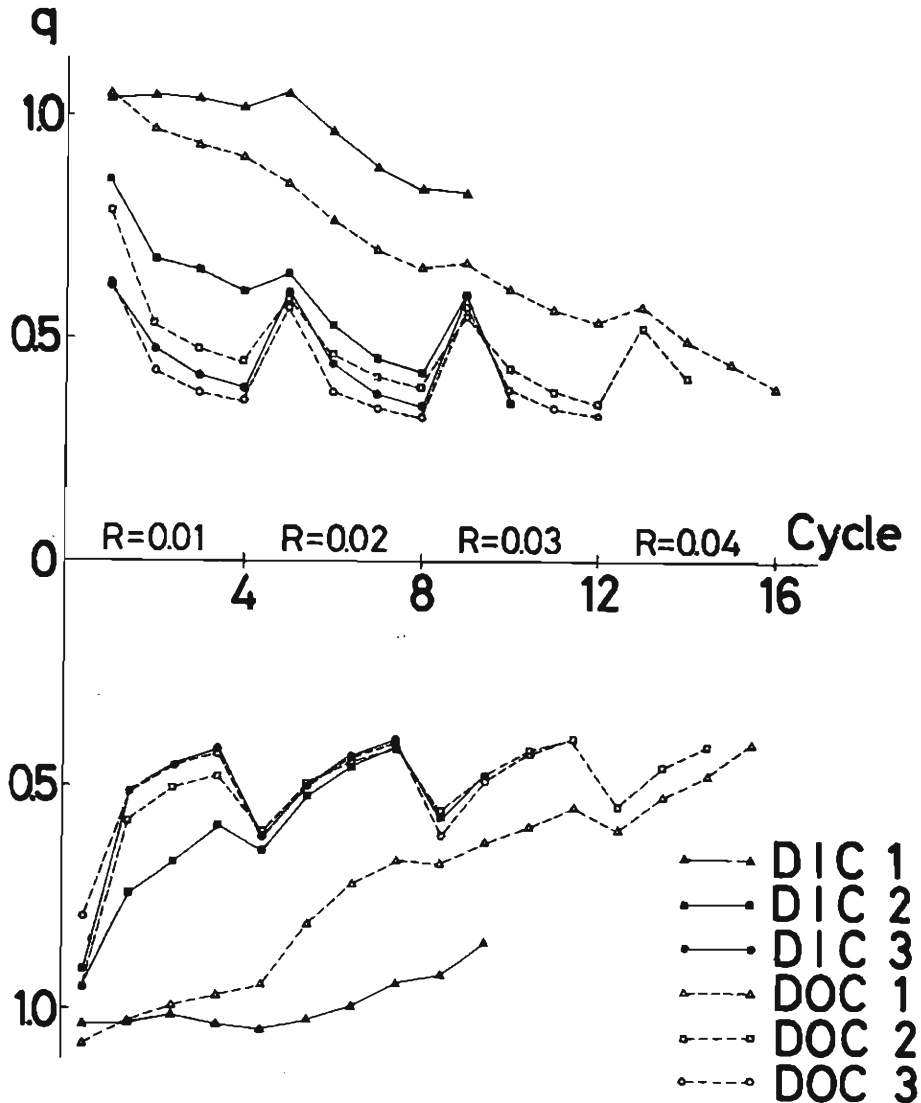The maximum load carrying capacity in each cycle of loading is examined as
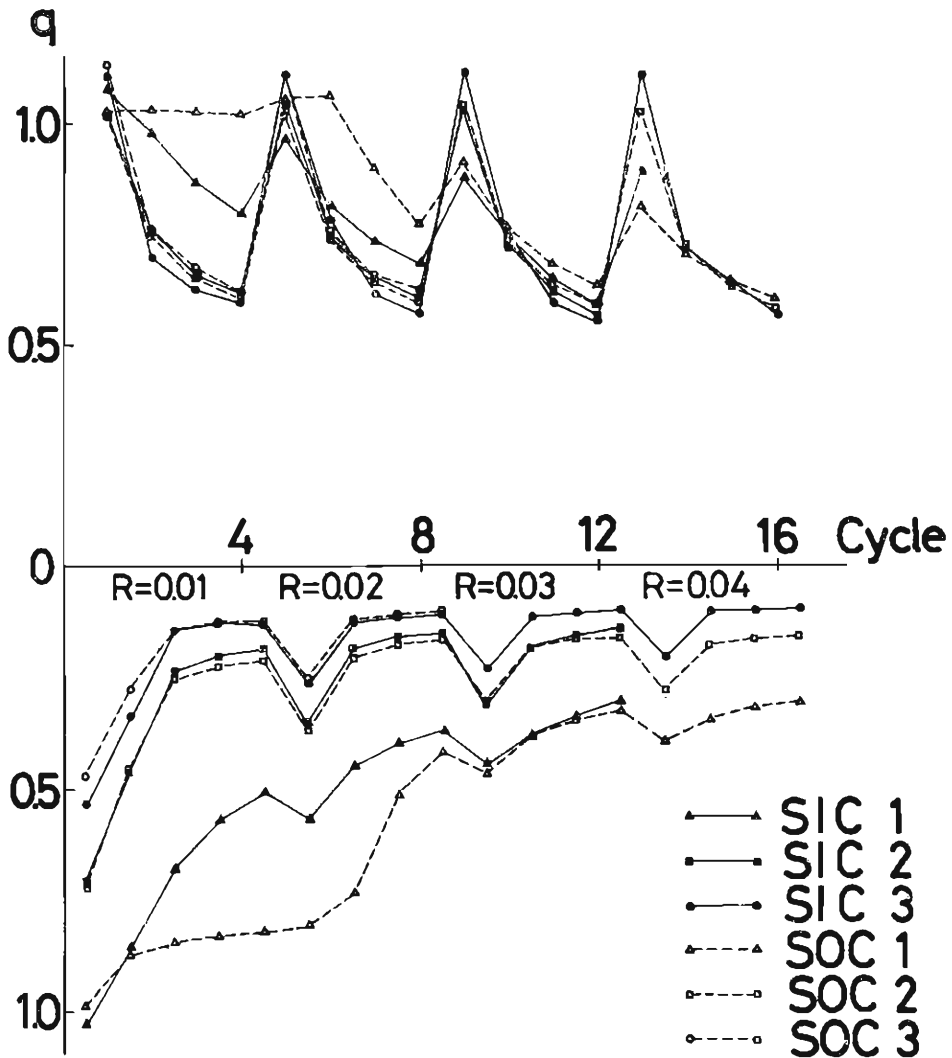


(a) Single brace

Fig. 27. Maximum load carrying capacity in each cycle of loading.

one of indices of the deterioration of hysteretic characteristics, and the results are shown in Fig. 27. The ordinate indicates the maximum load carrying capacity in each cycle and the abscissa shows the number of cycle.

Figure 27(a) is the result of single braces. The maximum tensile load carrying capacity in each cycle decreases hyperbolically under the cyclic loading in the constant displacement amplitude as the number of cycle increases. The maximum tensile load carrying capacity in the first cycle of loading in each amplitude is nearly equal to the yield load because the bar becomes almost straight at the load reversal point



(b)  Double brace

Fig. 27.  Maximum load carrying capacity in each cycle of loading.

in case of large slenderness ratio. In case of small slenderness, it is smaller than the yield load because the bar does not become straight at the load reversal point. After the second cycle of loading in each amplitude, the maximum tensile load carrying capacity is smaller as the slenderness ratio is larger. The maximum compression load carrying capacity is larger as the slenderness ratio is smaller.

Figure 27 (b) is the result of double braces. The maximum load carrying capacity in each cycle of loading also decreases hyperbolically under cyclic loading of the constant amplitude as the number of cycle increases. The maximum load carrying capacity-number of cycle relation is generally symmetric about the abscissa. The maximum strengths are always larger as the slenderness ratio is smaller.

### 4.3 Energy absorption

The energy absorbing capacity of a brace is one of the important factors which affects the behavior of braced structures during an earthquake. The deterioration of the energy absorbing capacity under cyclic loading is examined. The absorbing energy of the brace in a cycle of loading is nondimensionalized by the absorbing energy of an elastic-perfectly plastic model subjected to the identical displacement history (Fig. 28). The result is shown in Fig. 29. The abscissa is the number of loading cycles and the ordinate is the nondimensionalized absorbing energy $\zeta$. The decrease of the absorbed energy is remarkable at the second cycle of loading. The absorbing energy tends to decrease monotonically as the number of cycles increases, through the whole process of loading except the first cycle of loading in each displacement amplitude. The brace with a small slenderness ratio absorbs a larger amount of energy than the one with a large slenderness ratio, and the braces with the same slenderness ratio, for example *SIC* 2 and *SOC* 2, absorb almost equivalent energy in spite of the difference of the plane of deflection.

The deterioration of the energy absorbing capacity is observed even if the slenderness ratio is fairly small. For example, *DOM* 1, the monotonically loaded double brace with the slenderness ratio 22.5, behaves elastic-perfectly plastically.
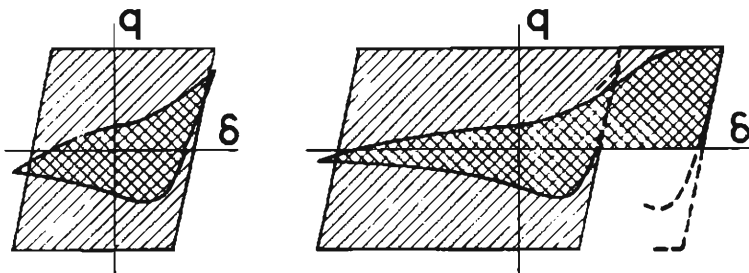


Fig. 28. Nondimensional absorbed energy.

however the absorbing energy of *DOC* 1, the repeatedly loaded one, in the fourth cycle of loading is about 80 % of that of the elastic-perfectly plastic model. In case of *SIC* 1, the single brace with the slenderness ratio 39. 6, it is only 50 % of that in the first cycle.

The nondimensional absorbing energy of a slip model, which represents the hysteretic characteristic of a brace with infinitely large slenderness ratio, is also shown in Fig. 29 by chain line. Braces absorb a pretty larger amount of energy than the slip model, even when the slenderness ratio is as large as 120.
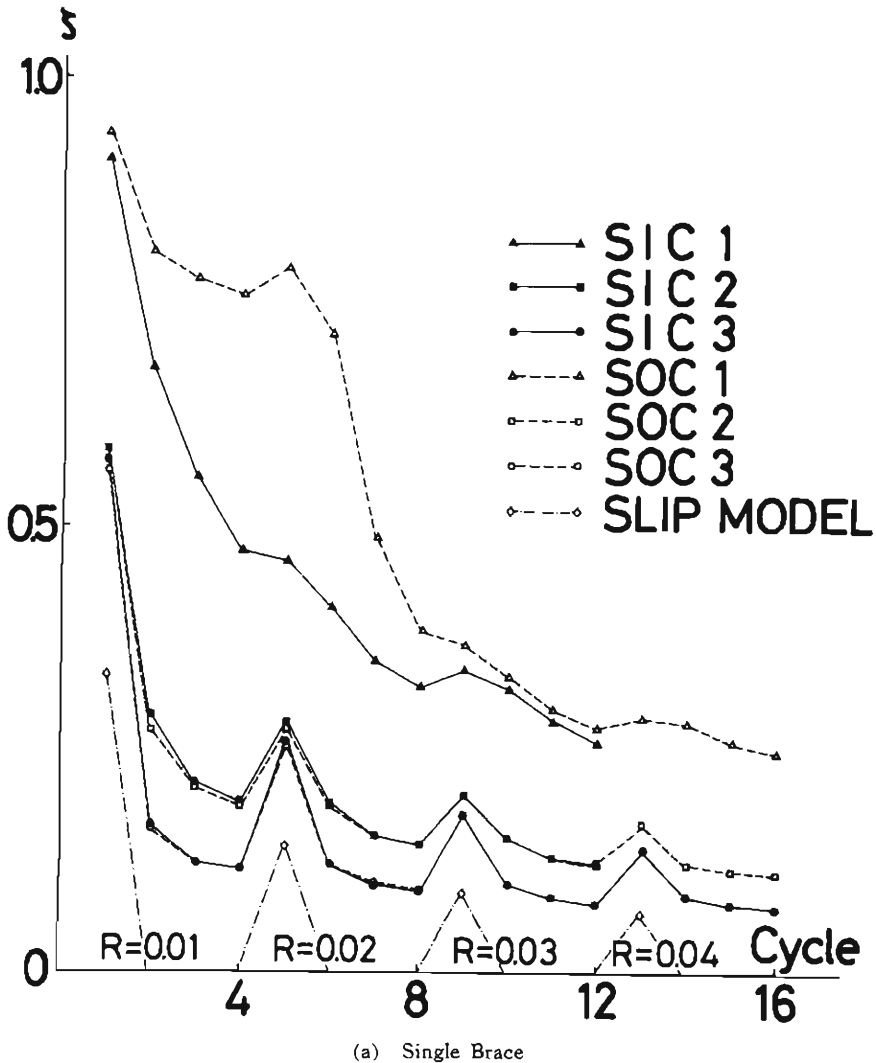


(a)  Single Brace

Fig. 29.  Nondimensional absorbing energy in each cycle of loading.

(b)  Double brace

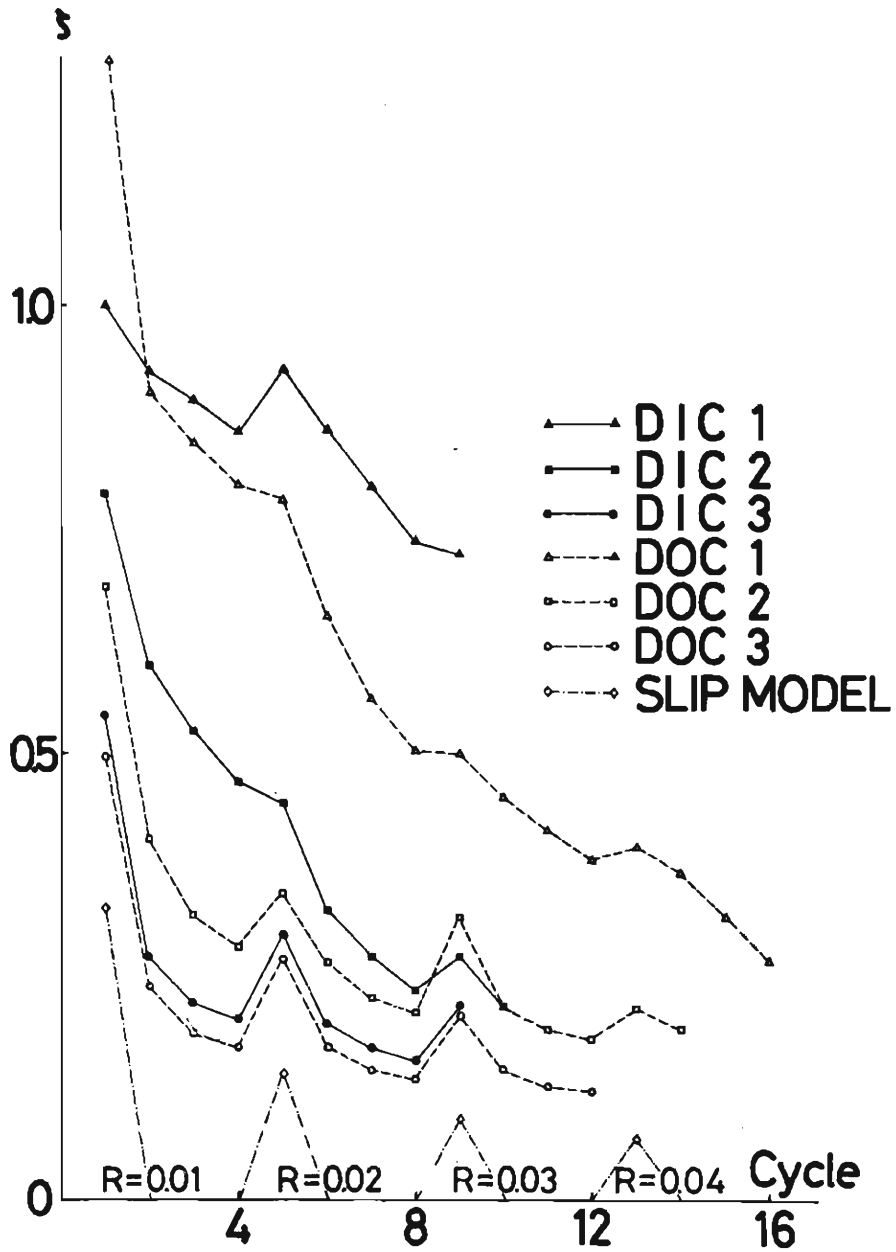Fig. 29.  Nondimensional absorbing energy in each cycle of loading.

## 4.4  The effect of the plane of lateral deflection

Since bracing members are subjected to not only longitudinal displacement but also transverse displacement in the plane of a frame due to the story drift of a frame the boundary conditions of a single brace deflecting in the plane of a frame is different to that deflecting out of the plane of a frame in the strict sense. However, as previously described, single braces which deflect in and out of the plane of a frame are equivalent in their energy absorbing capacity and their maximum load carrying capacity when their slenderness ratios are identical and they deflect about the weak axis of a cross section. The equivalence of behavior is also observed in the load displacement relationships as shown in Fig. 10 for monotonic loading and in Fig. 30 comparing *SIC* 2 to *SOC* 2 as an example of cyclic loading. In addition, a theoretical analysis[10] performed by the senior author relating with this test certifies that the effect of the compulsory end deformation due to the story drift of a surrounding frame is negligible and that single braces which deflect in the plane of a frame could be treated as a centrically loaded member unless the angle between a brace
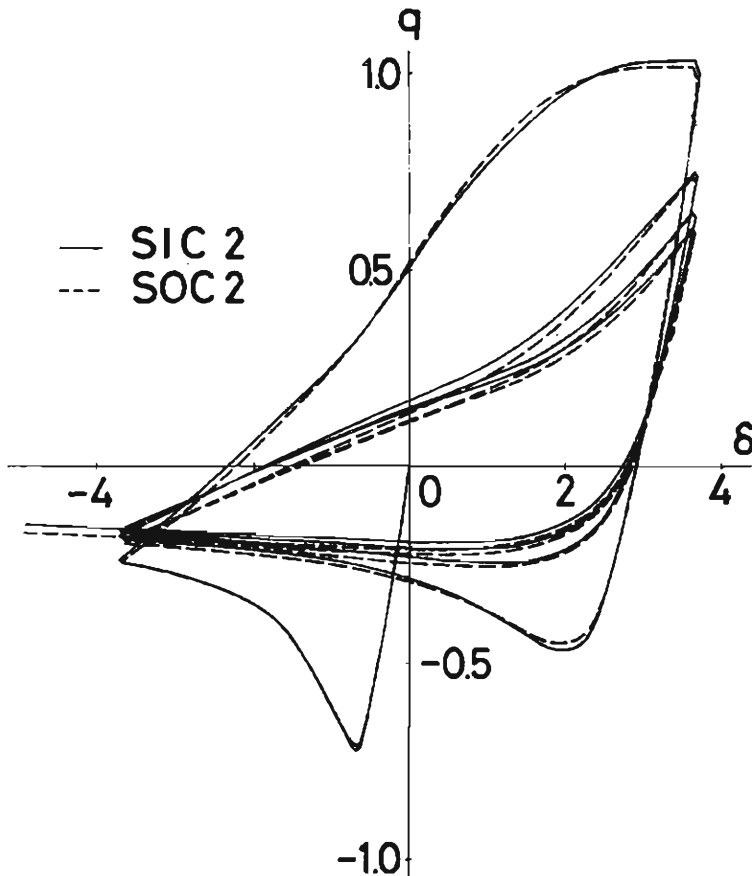


Fig. 30.  Comparison between *SIC* 2 and *SOC* 2.

and a beam is too large. Putting all accounts together, hysteresis loops of a single brace would be characterized by only the effective slenderness ratio.

In case of the double brace, the effective slenderness ratio is different if the buckling plane is different. It is about 0.6 times of the slenderness ratio of the single brace with the same length if double braces buckle in the plane of a frame, and it is about 0.7 times if they buckle out of the plane of a frame. The difference of the effective slenderness ratio depends on whether the tensile member restricts the rotation of the compression member at the mid-joint, or not. The effect of the plane of lateral deflection is not discussed here, because all effective slenderness ratios of double braces tested are different from each other.

## 4.5 The effect of the buckling plane

The specimens named *SOC* 1 and *DIC* 1 buckle about the strong axis of a cross section, unexpectedly. The effective slenderness ratio·about the strong axis is 40.2 for *SOC* 1 and 22.4 for *DIC* 1. The hysteretic loops of these specimens are quite different from those of braces which buckle about a weak axis. The behavior under cyclic loading is stable and the deterioration of the maximum load carrying capacity and the energy absorbing capacity is very small. The reasons why they have such hysteretic characteristics are explained in two different ways.

1° The effective slenderness ratio about strong axis buckling is smaller than that about weak axis buckling, when the length of the brace is identical. As described before, the decrease of the maximum load carrying capacity and the energy absorbing capacity becomes small as the slenderness ratio becomes small.

2° It has been certified by theoretical analysis of the authors[11] that the deterioration of hysteretic characteristics of the bar which buckles about a strong axis is smaller than that of the bar with the same slenderness which buckles about a weak axis.

In spite of the above mentioned observation, it is noticed that the bar which buckles about a strong axis originally comes to deflect about a weak axis after several cycles of loading. After that, the bar behaves as if it would have buckled about a weak axis originally.

4—6) Effect of local buckling

Local buckling takes place after several cycles of loading. The number of cycles when local buckling is found is shown in Table 3. Sudden deterioration of the load carrying capacity is not observed when local buckling is found, and the hysteretic loop does not change very much. However, the bending rigidity of the section at the locally buckled portion decreases and the bent bar has kinks, and soon cracks take place at the point of local buckling. The number of loading cycles when a crack is found is shown in Table 3. Cracks tend to occur earlier at the end of the bracing member, which is designed to buckle in the plane of a frame, where the notch effect is large due to the existence of the reinforcing plate.

Local buckling is significant in the sense that it induces cracks and the breakage of the member. Since the width-thickness ratio of rolled wide flange sections

which are usually used is larger than that of the tested specimen ($B/t_f = 5/0.6 = 8.3$), local buckling would take place easier in the practical design. The effect of width-thickness ratio on the breakage remains to be investigated in the future.

## 5. Concluding remarks

(1)   The effective slenderness ratio for buckling can be estimated by the use of the slope-deflection method, taking into account the secondary effect of axial force. According to the result of calculation, when bracing members are rigidly connected to a surrounding frame with relatively rigid members, the effective length of a single brace is a half of the bar length. It is about 0.6 times of the bar length for a double brace, which buckles in the plane of a frame, and it is about 0.7 times of the bar length for a double brace which buckles out of the plane of a frame.

(2)   The effective slenderness ratio used in this test are about 40-120 for the single brace, and about 22-84 for the double brace. The hysteretic characteristics of braces deteriorate even if the slenderness ratio is as small as 22. A certain amount of the compressive load carrying capacity can be expected even if the slenderness ratio is as large as 120.

(3)   Though the load carrying capacity is not changed very much by the occurrence of local buckling, local buckling is significant in the sense that it induces cracks and breakage of the member. The effect of width-thickness ratio on the breakage remains to be investigated in the future.

(4)   Though the boundary condition of a single brace is not simple i.e., a single brace is subjected to the compulsory end deformation due to the story drift of a surrounding frame, a single brace is substituted for simply supported bar whose length equals the effective length. The effective length for the behavior under repeated loading and for buckling is identical.

(5)   The effective slenderness ratio of a double brace for the behavior under repeated loading is regarded to be essentially different from the one for buckling.

(6)   Braces with a small slenderness ratio may buckle about the strong axis of a cross section unexpectedly. Their behavior under repeated loading is stable, and their load carrying capacity and energy absorbing capacity are larger than that of braces which have identical length and which buckle about a weak axis originally. However, after several cycles of loading, they come to deflect about the weak axis of a cross section, and they behave as if they would have buckled about a weak axis originally.

mental work and discussion.

# References

1) "A Guide to Earthquake Resistant Design of High Rize Building (a Proposal)" Building Letter, No. 95, June 1977, pp. 1–22 (in Japanese).

2) Wakabayashi. M., T., Nonaka, O. Koshiro and N. Yamamoto : An Experiment on the Behavior of a Steel Bar under Repeated Axial Loading, Disaster Prevention Research Institute Annuals, Kyoto University, No. 14 A, 1971, pp. 371–381 (in Japanese).

3) Igarashi, S., K. Inoue, M. Kibayashi and M. Asano : Hysteretic Characteristics of Steel Braced Frames-Part 1, the Behaviors of Bracing Members under Cyclic Axial Forces, Transactions of the Architectural Institute of Japan, vol. 196, June 1972, pp. 47–54 (in Japanese).

4) Wakabayashi, M., T. Nonaka, T. Nakamura, S. Morino and N. Yoshida : Experimental Studies on the Behavior of Steel Bars under Repeated Axial Loading, Disaster Prevention Research Institute Annuals, Kyoto University, No. 16 B, 1973, pp. 113–125 (in Japanese).

5) Yamada M. and B. Tsuji : Elasto-Plastic Behavior of Bracings under the Cyclic Axial Forces Part I : Analysis, Transactions of the Architectural Institute of Japan vol. 205, March 1973, pp. 31–35 (in Japanese).

6) Fujimoto, M., A. Wada, K. Shirakata and R. Kosugi : Nonlinear Analysis for K-Type Braced Frames, Transactions of the Architectural Institute of Japan, vol. 209, July 1973, pp. 41–51 (in Japanese).

7) Nonaka T. : An Elastic-Plastic Analysis of a Bar under Repeated Axial Loading, International Journal of Solid and Structures, vol. 9, No. 5 with Erratum in No. 10, 1973, pp. 569–580.

8) Higginbotham, A. B. : The Inelastic Cyclic Behavior of Axially Loaded Steel Members, Thesis Presented to the University of Michigan, at Ann Arbor, Michigan, 1973.

9) Shibata, M., T. Nakamura, N. Yoshida, T. Nonaka and M. Wakabayashi : Elastic-Plastic Bahavior of Steel Braces under Repeated Axial Loading, 5 th World Conference on Earthquake Engineering, Preprint No. 100, Rome, 1973, Proceedings (1974) pp. 845–848.

10) Wakabayashi, M., M. Shibata and H. Masuda : An Elastic-Plastic Analysis of a Brace Subjected to End Displacement, Disaster Prevention Research Institute Annuals, Kyoto University, No. 18 B, April 1975, pp. 143–154 (in Japanese).

11) Wakabayashi, M., T. Nonaka and N. Yoshida : An Elastic-Plastic Analysis of a Bar with Rotational Restraint under Repeated Loading, Annual Meeting of the Architectural Institute of Japan, 1976, pp. 1037–1038 (in Japanese).

12) Wakabayashi, M., C. Matsui and I. Mitani : Cyclic Behavior of a Restrained Steel Brace under Axial Loading, 6th World Conference on Earthquake Engineering, New Delhi, 1977, Preprint, vol. 11, pp. 189–194.

13) Wakabayashi, M., T. Nakamura, M. Shibata and N. Yoshida : Hysteretic Behavior of Steel Braces Subjucted to Horizontal Load due to Earthquake, 6 th World Conference on Earthquake Engineering, New Delhi, 1977, Preprint, vol. 11, pp. 195–200.

14) Kahn L. F. and R. D. Hanson : Inelastic Cycles of Axially Loaded Steel Members, A. S. C. E. ST 5, May 1976, pp. 947–959.

15) Tanaka S. and T. Shigenobu : Restoring Force Characteristics of Steel Members under Repeated Axial Loading (Analytical Model), Annual Meeting of the Architectural Institute of Japan, 1974, pp. 935–936.

16) Wakabayashi, M., T. Nonaka and M. Shibata : An Analysis on Elastic-Plastic Behavior of Steel Braces Subjected to Repeated Axial Force, in preparation.

17) Wakabayashi M. and B. Tsuji : Experimental Investigation on the Behavior of Frames with and without Bracing under Horizontal Loading, Bulletin of Disaster Prevention Research Institute, Kyoto University, vol. 16, Part 2, No. 112, Jan. 1967, pp. 81–94.

18) Fujimoto, M., H. Hakura and Y. Matsumoto : Model Experiment of Braced Steel Rahmen under Repeated Loading, JSSC, vol. 6, No. 55, June 1970, pp. 15-27.

19) Fujimoto et al. : Elastic-Plastic Bahavior of Braced Steel Rahmen under Repeated Horizontal Loading, (Part 2-Part 4, Experiment of K-Type Braced Rahmen I—III), Annual Meeting of the Architectural Institute of Japan, 1971, pp. 397-400, and 1972, pp. 1373-1374.

20) Fujimoto et al. : Elastic-Plastic Bahavior of Braced Steel Rahmen under Repeated Horizontal Loading, (Part 8, Experiment of K-Type Braced two Storied Rahmen (IV)), Annual Meeting of the Architectural Institute of Japan, 1973, pp. 1053-1054.

21) Fujimoto et al. : Elastic-Plastic Behavior of Braced Steel Rahmen under Repeated Horizontal Loading, (Part 9, Experiment of X-Type or K-Type Braced one or two Storied Rahmen), Annual Meeting of the Architectural Institute of Japan, 1974, pp. 971-972.

22) Wakabayashi, M., C. Matsui, K. Minami and I. Mitani : Inelastic Behavior of Full Scale Steel Frames, Disaster Prevention Research Institute Annuals, Kyoto University, vol 13A, 1970, pp. 329-363.

23) Yamada, M., B. Tsuji and S. Nakanishi : Elasto-Plastic Behavior of Braced Frames under Cyclic Horizontal Loading, 6th World Conference on Earthquake Engineering, New Delhi, 1977, Preprint, vol. 9, pp. 77-82.

24) Suzuki, T., K. Tamamatsu, I. Kubodera and K. Okuda : Experimental Study on the Elasto-Plastic Behavior of Tensile Braced Frames (Studies on Seismic Resistivity of Low Steel Structures, Part 1), Transactions of the Architectural Institute of Japan, vol. 228, Feb. 1975, pp. 57-64.

25) Wakabayashi M. et al. : Experimental Studies on Braced Steel Frame, Sumitomo Metals, vol. 28, No. 3, Jul. 1976, pp. 80-100.

## Notations

$A$ : Cross sectional area

$B$ : Width of flange

$D$ : Depth of cross section

$E$ : Young's modulus

$h = l/\sqrt{2}$, clear height of column

$I$ : Moment of inertia

$l$ : Length of a bracing member

$N$ : Axial force of a bracing member

$N_y$ : Yield axial force of a bracing member

$Q$ : Horizontal load

$Q_y$ : Yield horizontal load ($\sigma_y A/\sqrt{2}$ or $\sqrt{2}\,\sigma_y A$ for a single or a double brace, respectively)

$q = Q/Q_y$

$R = \Delta/h$, rotation angle of column

$t_w$ : Thickness of web

$t_f$ : Thickness of flange

$V_s$ : Lateral deflection about strong axis of cross section at mid-length of the bar

$V_w$ : Lateral deflection about weak axis of cross section at mid-length of the bar

$\varepsilon_y = \sigma_y/E$, yield strain

$\sigma_y$ : Yield stress

$\Delta$ : Horizontal displacement

$\Delta_A$ : Axial displacement

$\Delta_y = \sqrt{2}\,\varepsilon_y l$, yield horizontal displacement

$\delta = \Delta/\Delta_y$

$\lambda$ : Effective slenderness ratio